Transactions, SMiRT-24
BEXCO, Busan, Korea - August 20-25, 2017
Division VI (Paper ID 06-14-05)

INVESTIGATION OF ACCIDENT THERMAL EFFECTS ON SEISMIC PERFORMANCE OF STRUCTURAL WALLS

Saahastaranshu R. Bhardwaj[1], Kadir C. Sener[2], and Amit H. Varma[3]

[1] Ph.D. Candidate, Civil Engineering, Purdue University, West Lafayette, IN, USA
[2] Research Engineer, Civil Engineering, Purdue University, West Lafayette, IN, USA
[3] Professor, Civil Engineering, Purdue University, West Lafayette, IN, USA

ABSTRACT

The Fukushima nuclear accident of 2011 has highlighted the importance of designing safety-related nuclear facilities for combination of accident thermal scenarios, and design basis and beyond design basis shaking. This paper presents the preliminary results from a research project, the overall goal of which is to develop knowledge-based design guidelines for safety related nuclear facilities subjected to combined accident thermal conditions and seismic loading. Experimental results investigating the effects of accident thermal conditions on the seismic (in-plane shear) behaviour of steel-plate composite (SC) walls are briefly discussed. Preliminary results from SC wall and SC wall piers indicate that thermal loads reduce the stiffness of walls. The reduction in stiffness is attributed to extensive concrete cracking due to non-linear thermal gradients through the thickness of the specimens. SC wall piers subjected to idealized thermal load histories did not experience/exhibit significant degradation in strength and post-peak performance. Heated SC wall specimens also achieved its design in-plane shear strength, with a safety margin of 30%. The results from the preliminary testing indicate that there is no significant effect of thermal loads (accident thermal temperatures ranging from 300°F to 450°F) on the SC wall strength and post-peak response.

INTRODUCTION

The Fukushima nuclear accident of 2011 has highlighted the importance of designing safety-related nuclear facilities for combination of accident thermal scenarios, and design basis and beyond design basis shaking. While the probability of both events occurring simultaneously is low, severe environmental conditions may trigger accident thermal loading. Additionally, subsequent aftershocks (potentially as intense as the main shock) may occur during the accident thermal event. Current design codes and standards in the United States and abroad provide little/no guidance for including the effects of accident thermal loading on seismic behavior (stiffness, strength, ductility or reserve margin) of structures.

Prior research has focused on either seismic behavior or accident thermal loading but not both in combination. This combination of accident thermal loading and safe shutdown earthquake (SSE) also present a significant design challenge for Small Modular Reactors (SMRs) and Advanced Light Water Reactors (ALWRs) because postulated accident scenarios may cause higher elevated temperatures for longer durations in their small and/or constrained spaces. The regulator may potentially require extensive technical information and evidence of safety, which may jeopardize the licensing schedule.

There is a need to develop design guidelines (based on experimental and numerical studies) for safety-related nuclear facilities subjected to combined accident thermal conditions and seismic loading. The authors have initiated a research project (sponsored by US Department of Energy) focusing on investigating the effect of accident thermal loads on the seismic behaviour of structural walls. The research program includes the following tasks, (i) identification of parameters influencing behaviour, and finalization of accident thermal conditions, (ii) experimental evaluation of the effects of accident thermal conditions on the seismic (in-plane shear) behavior of steel-plate composite (SC) and reinforced concrete (RC) walls, (iii) development and benchmarking of numerical models for predicting experimental results and observed

behavior, (iv) comprehensive analytical parametric studies to evaluate the influence of various parameters and ranges, and (v) development of design guidelines and analysis recommendations for design basis and beyond-design-basis events involving combination of accident thermal and seismic loading conditions.

This paper presents the test matrix, the loading and heating protocol, instrumentation, and test set up for the specimens. Specimen design and details, expected behaviour, and preliminary experimental observations for SC specimens are also discussed.

TEST MATRIX

The test program has been set up to investigate the effect of accident thermal loads on the seismic response of SC and RC walls. Table 1 and Table 2 present the test matrices for SC and RC specimens respectively. SC test specimens include SC wall piers (without flange walls) and SC walls (with flanges). There will be one ambient control specimen (SC-WP-C and SC-W-C) and one heated specimen (SC-WP-H and SC-W-H) each for SC wall pier and SC wall specimens. The RC specimens consist of two control specimens and two heated specimens, one each for ambient and heated thermal conditions. The specimens have 1% and 2% longitudinal and transverse reinforcement. The in-plane response for control (ambient) and heated specimens will be compared to investigate the effects of accident thermal loads on the stiffness, peak strength and post-peak behavior of these wall specimens.

Table 1: Test Matrix for SC Specimens

Specimen ID	Specimen dimensions (in.)			Faceplate thickness (in.)	Reinf. Ratio %	End plate thickness (in.)	Tie Spacing (S), in.
	Thickness	Height	Length				
SC-WP-H	12	36	60	0.1875	3.1	No end plate	6
SC-WP-C							
SC-W-H	10	36	48	0.1046 (12ga)	2.1	0.75	5
SC-W-C							

Table 2: Test Matrix for RC Wall Specimens

Specimen ID	Wall thick. T (in.)	Height (in.)	Length (in.)	Rebar size & Spacing (Long. And Transverse)	Reinforcement ratio %
RC-1-H	10	36	60	#4@4in.	1%
RC-1-C					
RC-2-H				#6@4in.	2%
RC-2-C					

SPECIMEN DESIGN AND EXPECTED BEHAVIOR

The in-plane behavior of SC wall piers is different than that of labyrinthine SC walls. While the SC walls (with flanges) resist the in-plane flexure through the flanges, and in-plane shear through the web; SC wall piers are subject to the combination of in-plane moment and in-plane shear (since there are no flanges). The in-plane shear behavior of SC wall panels and walls with flanges or cross-walls, was developed by Ozaki et al. (2004) and extended by Varma et al. (2011). The in-plane behavior can be estimated as the tri-linear shear force–strain (Sxy-γ) curve. Seo et. al. (2016) verified the tri-linear curve using a large in-plane shear test experimental database, and observed that AISC N690s1 equations predict the in-plane strength conservatively. Kurt et al. (2016) and Epackachi et al. (2015) conducted experimental and numerical studies to understand the in-plane shear behavior of SC wall piers. The authors observed that SC wall piers with aspect ratios greater than or equal to 0.6 failed in in-plane flexure. The failure was governed by cyclic

yielding and local buckling of faceplates, concrete crushing, and eventual faceplate fracture. Luna et al. (2015) observed that the in-plane shear behavior of squat RC walls is controlled by in-plane shear. The authors tested low-aspect ratio (0.5 to 1.0) RC walls (reinforcement ratios ranging from 0.33% to 1.5%) and observed that all specimens failed in diagonal tension or diagonal compression. Based on these observations, SC wall pier specimens (aspect ratio 0.6) are designed to have flexure controlled behavior. Low aspect ratio of RC wall (aspect ratio of 0.6) specimens ensures that the response is governed by in-plane shear behavior.

The SC wall (aspect ratio of 0.75) specimens are designed to fail in in-plane shear mode without premature buckling of the faceplates. End (flange) plates are added to the design to increase the flexural strength and have the governing failure mode of walls to be shear failure. The thickness of the end plates is designed to have flexural strength to be larger than shear strength. Japanese researchers (Kitajima et al. 2015) have tested similar SC wall specimens with end plates, which failed in in-plane shear mode. These specimens were modeled and analyzed (Sener et al., 2017) to develop benchmark models that are later used for predicting the behavior and response of the specimen in the proposed test matrix. The monotonically loaded specimen tested by Kitajima et al. (2015) in ambient condition (Specimen No. 2) was modeled using finite element method for developing benchmark models. The lateral shear force vs. lateral deformation response of Specimen No. 2 (Kitajima et al. 2015) is compared with the numerical analysis results in Figure 1. The figure also includes horizontal lines corresponding to shear and flexural strength of the wall. The shear strength was calculated using the in-plane shear strength equations in AISC N690. The flexural strength was calculated based on section analysis assuming yielding in the end-plates, faceplates in the elastic range and rectangular block for concrete in compression. The comparison indicates that the experimentally measured stiffness and strength is predicted accurately by the numerical analysis results. The benchmarked models were then used to predict the behavior and response of the designed SC wall specimens. The end plate thickness was used as a parameter to design the specimen to have flexural strength larger than shear strength and to have in-plane shear as the governing failure mode. Figure 2 shows the lateral shear force – lateral deformation response of the proposed SC wall specimens. Three different thicknesses for end plates were used in the models (0.50, 0.75 and 1.00 in.). The response comparisons indicate that the 0.75-inch end-plate thickness is providing sufficient flexural capacity that the specimen fails in shear failure.

Bhardwaj et al. (2015) discussed the effect of operating and accident thermal loads (from postulated pipe break scenarios) on the structural behavior of wall structures, and the evolution of through thickness non-linear thermal gradients for accident thermal loads. During the first few hours (up to one day) of the thermal accident, structural members are subjected to significantly nonlinear thermal gradients over the thickness. These nonlinear thermal gradients induce significant concrete cracking due to internal or self-restraint. After the first few hours (up to one day) of the accident, the thermal gradients become relatively uniform through the thickness. The concrete cracks, produced during the first few hours due to self-restraint, close due to the uniformity of the temperatures through the thickness. The uniform temperatures are lower than the maximum values reached earlier. However, the concrete will never regain its uncracked stiffness for mechanical loads.

For combined thermal and seismic loads, the concrete cracking due to non-linear thermal gradient will reduce the concrete contribution to the specimen stiffness. As the thermal gradient becomes uniform with time, the concrete cracks will close and the stiffness of the specimen is expected to increase. For higher surface temperatures (around 450°F), the steel elastic modulus will reduce by about 15%, which would further reduce the stiffness of the specimen (in addition to the reduction due to concrete cracking). Therefore, accident thermal temperatures are expected to result in a softer response of the specimen. Additionally, pinching in the force-drift response is expected of the specimens (especially for shear controlled specimens) as the specimen will be softer before the concrete cracks close and stiffen up thereon. However, the accident thermal temperatures (typical surface temperatures ranging from 300°F to 450°F) are not expected to reduce the strength of the specimens (although the peak load is expected to be reached at higher drifts in comparison to unheated specimens). This is because these temperature magnitudes are not expected to lead to any significant changes in the material and structural response of the walls.

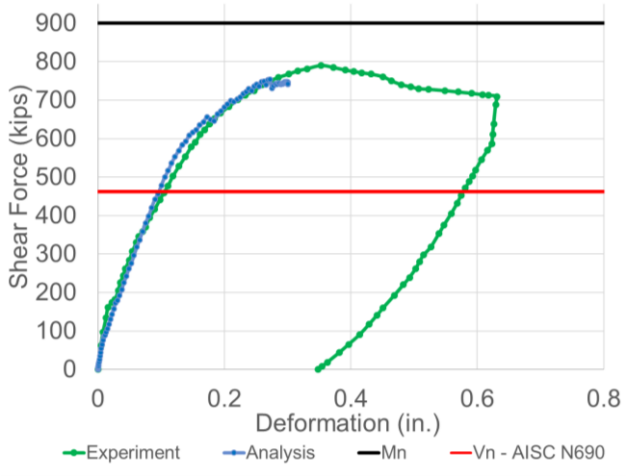

Figure 1. Comparison of Lateral Load-Deformation Response of Specimen No. 2 from Kitajima et al. (2015)

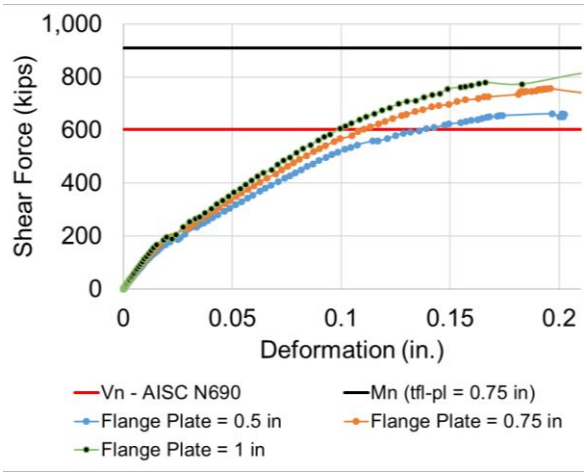

Figure 2. Comparison of Lateral Load-Deformation Response of Proposed SC Wall Specimens SC-W-H/C

LOADING AND HEATING PROTOCOL, INSTRUMENTATION, AND TEST SET UP

The loading and heating protocol is summarized in Table 3. The heated specimens were subjected to two surface temperature amplitudes (300°F and 450°F), and subjected to force cycles at heating durations of 1 hour and 3 hours. The temperature amplitudes are idealized versions of typical surface time temperature histories for containment internal structures (CIS) for postulated pipe break scenarios as obtained from public domain documents. The formulation of ideal time-temperature curves is discussed in Sener et al. (2015). Based on the discussion in Bhardwaj et al. (2015), 1-hour heating duration was chosen to obtain a non-linear thermal gradient (resulting in extensive concrete cracking) through the cross-section. The 3-hour heating duration will result in more uniform temperatures through the cross-section (reducing the crack widths). These temperature durations were scaled down for the specimens (1/3 to 1/4 scaled specimens) to result in through thickness temperature profiles similar to those observed in physical wall structures, as discussed in Sener et al. (2015). The evolution of non-linear thermal gradients through the thickness for Specimen SC-WP-H is shown in Figure 4. The specimens were allowed to cool to ambient condition after completing the load cycles at 3 hours of heating, and heated/loaded to the next temperature/load level.

The first three load cycles were performed at ambient condition and the load levels corresponded to 25, 50 and 75% of the calculated/estimated specimen strength, F_n (Cycles 1, 2, 3). For SC-WP-H, F_n is the force corresponding to expected yield moment, calculated as discussed in Kurt et al. (2016). For, SC-W-H specimen, F_n is the force corresponding to nominal shear strength of the specimen, based on AISC N690 (AISC, 2015) Equation A-N9-19. The initial cycles were performed to investigate the ambient behavior of the wall pre-post concrete cracking and before any yielding in steel, and to determine the differences in behavior due to heating cycles. The ambient cycles were followed with the heated load cycles by heating the faceplate surface temperatures to 300°F and for 1 and 3 hours (Cycles 4,5). Similar load cycles were conducted for the surface temperature of 450°F in Cycles 6 and 7. The test was switched to displacement controlled loading in the remaining load cycles. The yield displacement (Δ_y) is estimated as the displacement corresponding to the expected strength (F_n) of the specimen, based on the secant stiffness observed in Cycles 6 and 7. The test continued with displacement cycles at $1.0\Delta_y$ (Cycles 8,9), $1.5\Delta_y$ (Cycles 10,11). The loading and heating cycles following the listed cycles were decided based on the post-peak response of the specimens. For specimen SC-W-H, since the ambient specimen had not been tested yet, additional ambient loading cycles were performed at target force/displacement levels of $1.0\Delta_y$ and $1.5\Delta_y$. These ambient cycles were performed after the heated cycles at these load/displacement levels to determine the changes in stiffness due to heating. Figure 3 presents the loading and heating history for specimen SC-

WP-H. The history is consistent with the loading and heating protocol presented in Table 3. Post $1.5\Delta_y$ cycles, the specimen was subjected to $2.0\Delta_y$ with the surface temperatures maintained at 450°F for a duration of 4 hours.

Table 3: Loading and Heating Protocol

Force Cycle No.	Surface Temperature	Heating Duration	Target Force/ Displacement Level
1	Ambient	-	$0.25F_n$
2	Ambient	-	$0.5\ F_n$
3	Ambient	-	$0.75\ F_n$
4	300°F	1 hr	$0.75\ F_n$
5	300°F	3 hr	$0.75\ F_n$
6	450°F	1 hr	$0.75\ F_n$
7	450°F	3 hr	$0.75\ F_n$
8	450°F	1 hr	$1.0\ \Delta_y$
9	450°F	3 hr	$1.0\ \Delta_y$
10	450°F	1 hr	$1.5\ \Delta_y$
11	450°F	3 hr	$1.5\ \Delta_y$

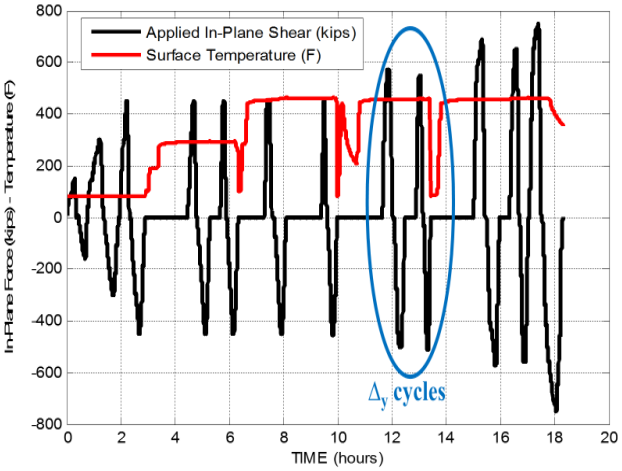

Figure 3. Applied Mechanical and Thermal Loading Histories for Specimen SC-WP-H

The specimens were instrumented with (i) displacement sensors to calculate in-plane drift response and base sliding corrections, (ii) rotation sensors at the base to determine base rotation corrections, (iii) high temperature strain gauges for strain measurements on steel faceplates and flange plates, and (iv) thermocouples for surface temperature measurements to obtain through thickness temperature profiles. For specimen SC-WP-H, Figure 4 presents the temperature profiles through the wall cross-section generated using the readings from the thermocouples embedded in the concrete infill. Typical temperature profiles obtained from the experimental measurements are shown for 300°F and 450°F surface temperature cases, respectively.

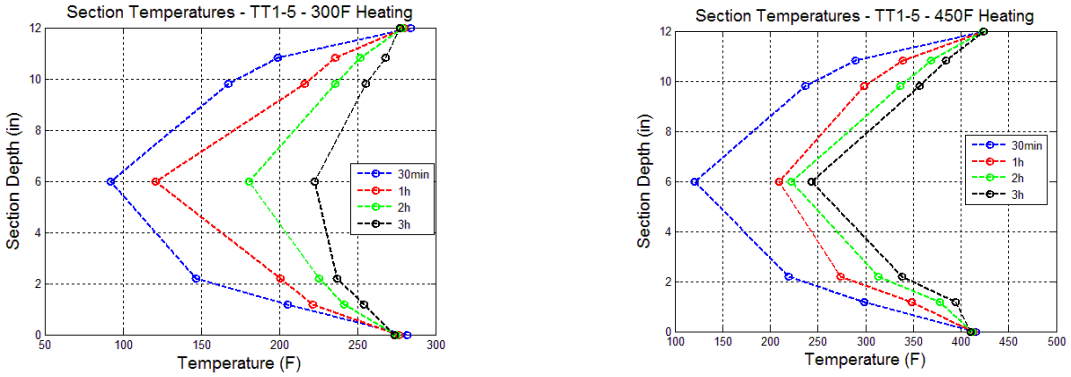

a) 300°F b) 450°F

Figure 4. Specimen SC-WP-H: Temperature Profiles Through Cross-Section

Figure 5 shows the test setup for the SC specimens. Cyclic in-plane loading was applied by two double acting actuators (Enerpac RR50012). The actuators are connected to the loading beams. The in-plane loading beams apply the load to the specimen through end bearing, and bearing at the holes in the specimens. Figure 5b) shows the ceramic heaters set up for specimen SC-WP-H.

SUMMARY OF EXPERIMENTS

This section summarizes the experimental observations for SC specimens (SC wall piers and SC walls). The effect of accident thermal loads on the stiffness and strength of the specimens is briefly discussed.

SC Wall Pier Specimens

The specimens SC-WP-C and SC-WP-H consisted of two steel faceplates with concrete infill, and was constructed by assembling the steel faceplates using tie bars (shown in Figure 5a). Faceplates of the specimen are welded to the baseplate that is anchored to the foundation. Shear studs on the steel faceplates were spaced to prevent premature local buckling of the faceplates, i.e., buckling of faceplates before yielding. Figure 6 presents the force-displacement response for specimens SC-WP-C (ambient) and SC-WP-H (heated). It is observed that the heating cycles do not affect the strength of the SC wall pier specimens (peak loads for SC-WP-H and SC-WP-C push cycles are within 5%). Additionally, the post-peak behavior of the two specimens was similar. Both the specimens underwent faceplate yielding, followed by compression buckling (as shown in Figure 8 for SC-SP-H), and failed due to faceplate rupture. The extent of damage in SC-WP-H at failure is presented in Figure 10 (SP-WP-C is discussed in detail by Kurt et al., 2016).

However, the thermal loads do reduce the stiffness of the specimens. In Figure 6, comparison of cycles 6 and 7 (same peak load) for heated and ambient specimens confirm the reduction in stiffness for the heated specimen. The extent of cracking for the similar load levels was higher in SC-WP-H. The reduction in stiffness of the specimen as it is subjected to thermal loading cycles is also apparent from Figure 7, which shows the percent stiffness degradation in comparison to the ambient specimen (Cycle 3, 0.75 F_n). The stiffness (secant stiffness) is calculated between points of zero load and peak load for each half cycle. To look further into the stiffness degradation, the lateral load response of the ambient and heated specimens during the final two displacement cycles, $1.5\Delta_y$ and $2.0\Delta_y$, is compared in Figure 9. The response comparisons show that the heated specimen had lower stiffness during the $1.5\Delta_y$ load cycle, which indicates that the heated specimen had more extensive yielding in the steel faceplates, and concrete cracking. The ambient specimen experienced local buckling and extensive yielding in the $1.5\Delta_y$ cycle, therefore the stiffness comparisons in the final cycle ($2.0\Delta_y$) were similar for both the heated and ambient cases.

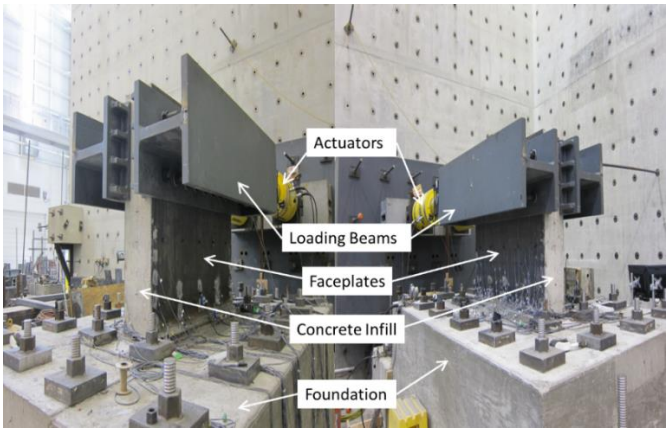

a) Test Set up (without heaters)

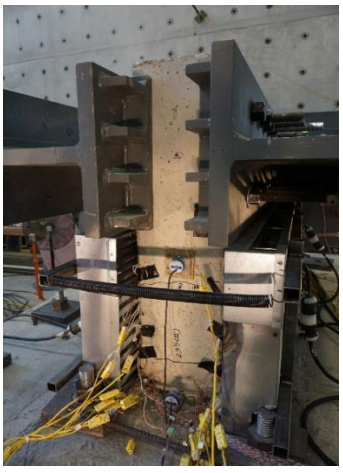

b) Heaters Installed

Figure 5. Test Set up for SC Wall Pier Specimens

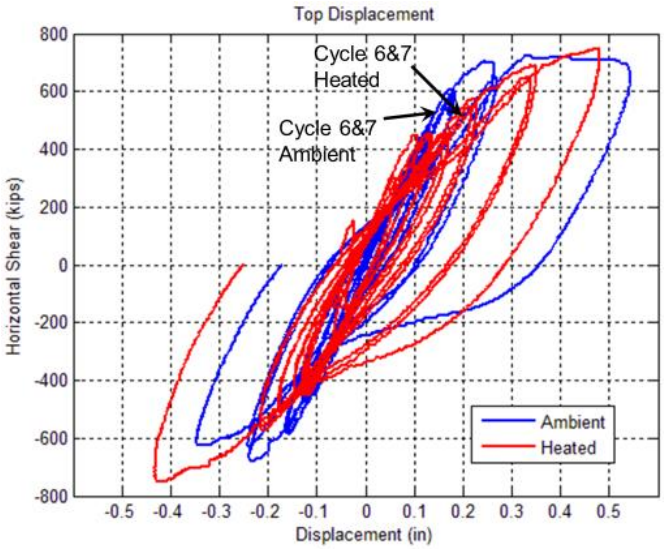

Figure 6. Complete Lateral Load Response Comparison of Ambient and Heated SC Wall Pier Specimens

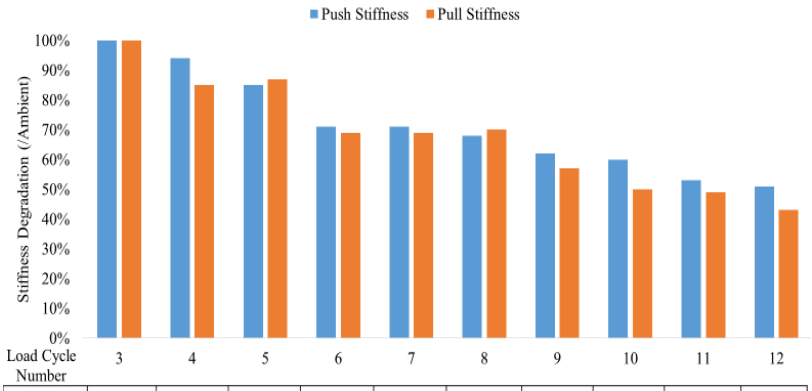

Load Cycle Number	3	4	5	6	7	8	9	10	11	12
Force	$0.75F_n$	$0.75F_n$	$0.75F_n$	$0.75F_n$	$0.75F_n$	Δ_y	Δ_y	$1.5\Delta_y$	$1.5\Delta_y$	$2\Delta_y$
Temp.	Ambient	300°F	300°F	450°F	450°F	450°F	450°F	450°F	450°F	450°F
Duration	-	1hr	3hr	1hr	3hr	1hr	3hr	1hr	3hr	4hr

Figure 7. Stiffness Degradation During Load Cycles

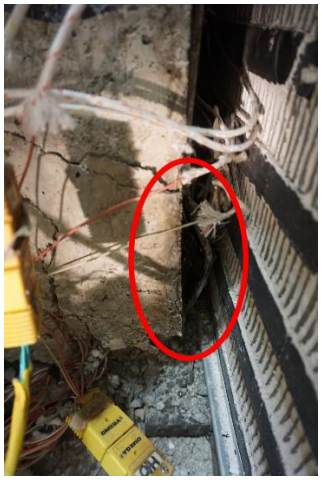

Figure 8. Local Buckling of Steel Faceplates in Compression

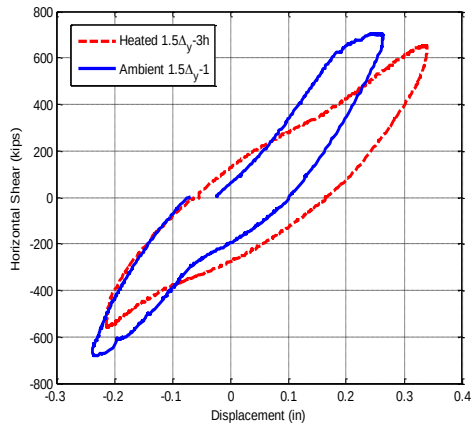

a) $1.5\Delta_y$ Cycles

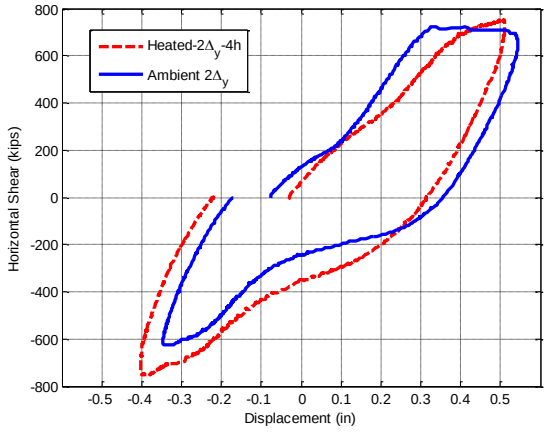

b) $2\Delta_y$ Cycles

Figure 9. Comparison of SC-WP specimens at large displacement cycles

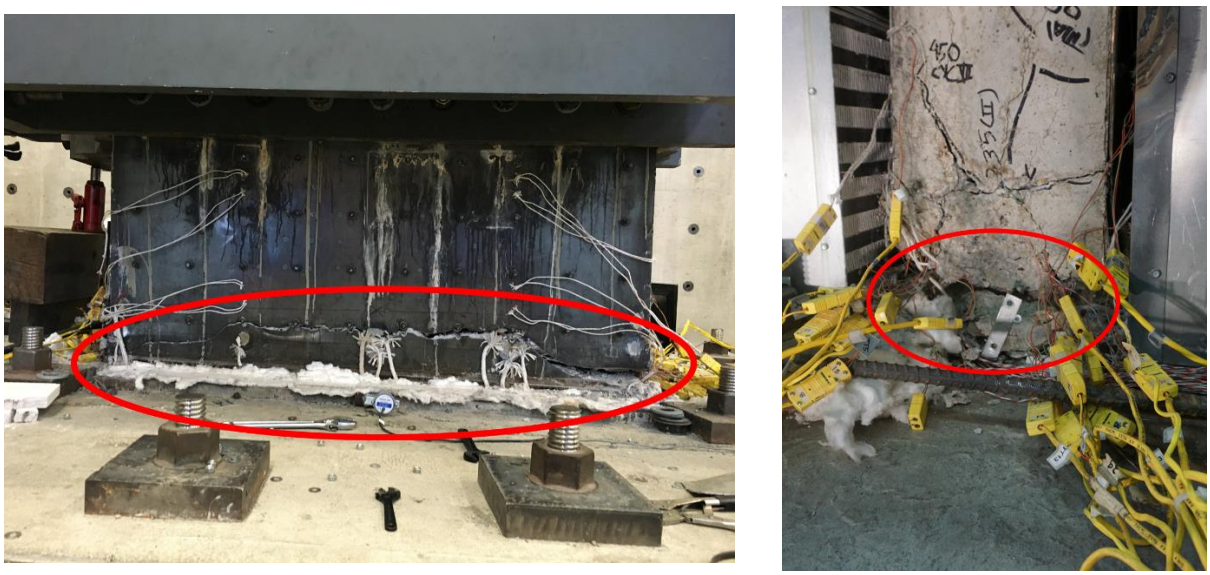

a) Faceplate Rupture

b) Concrete Cracking and spalling

Figure 10. Specimen SC-WP-H at failure

SC Wall Specimens

Specimen SC-W-H was also subjected to the loading and heating protocol presented in Table 3. Figure 11 presents the force-drift response of specimen SC-W-H. The design in-plane shear strength for the specimen per AISC N690 (Equation A-N9-19) is plotted. It is observed that the specimen develops the design shear strength, and the peak in-plane shear force for the specimen was about 30% higher than the design strength. The pinching behavior observed in the post-yield cycles indicates the crack opening-closing in concrete. In addition, the thermal loads reduce the stiffness of the specimen. Figure 12 presents the force-displacement responses for ambient and heated cycles at 0.75 F_n load level. It is observed that there is a reduction in the stiffness of the specimen when subjected to heating cycles. Figure 13 shows the heated and ambient cycles for Δ_y cycles. The ambient cycle was performed after the heated cycles (the specimen was allowed to cool down). The stiffer response for the ambient cycle confirms the reduction in stiffness due to thermal loads. The degradation of the specimen secant stiffness over the cycles is presented in Figure 14. It is observed that thermal loading leads to drastic reduction in the secant stiffness of the specimens. The stiffness (secant stiffness) is calculated between points of zero load and peak load for each half cycle.

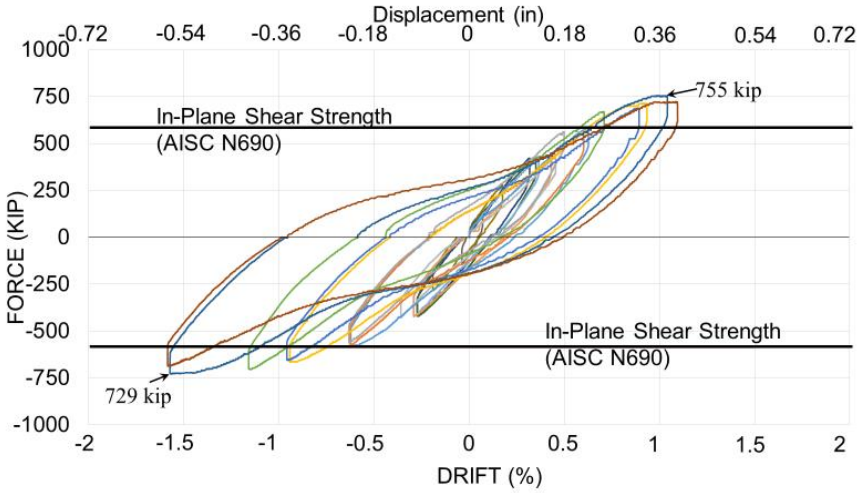

Figure 11. Force Drift/Displacement Plot for Specimen SC-W-H

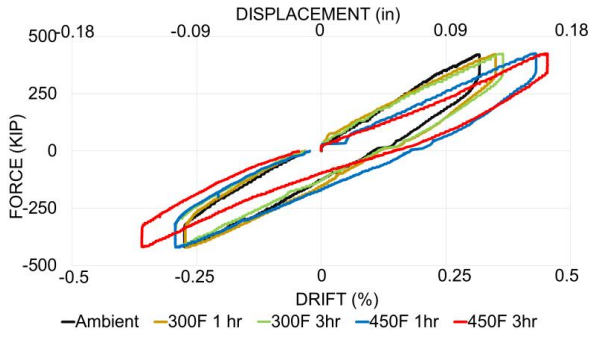

Figure 12. Force-displacement for 0.75Fn cycles for Specimen SC-W-H

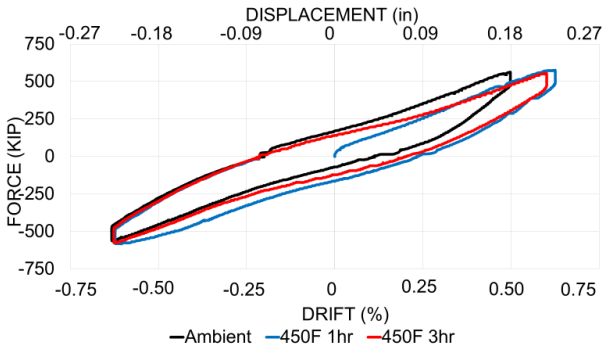

Figure 13. Force-displacement for Δ_y cycles for Specimen SC-W-H

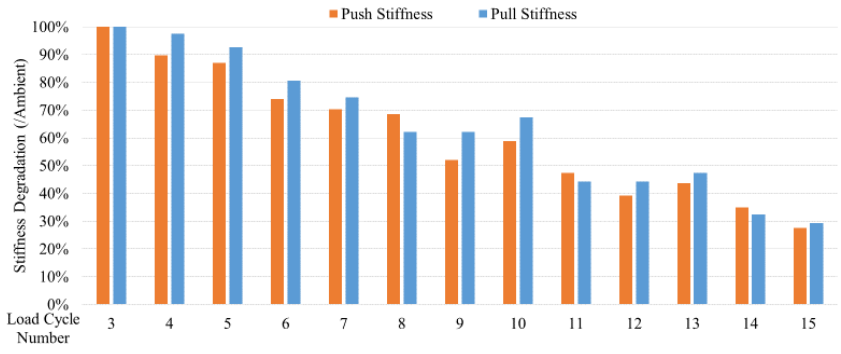

Force	0.75 F_n	0.75 F_n	0.75 F_n	0.75 F_n	0.75 F_n	Δ_y	Δ_y	Δ_y	1.5Δ_y	1.5Δ_y	1.5Δ_y	2Δ_y	2Δ_y
Temp.	Ambient	300°F	300°F	450°F	450°F	450°F	450°F	Ambient	450°F	450°F	Ambient	450°F	450°F
Duration	-	1hr	3hr	1hr	3hr	1hr	3hr	-	1hr	3hr	-	1hr	3hr

Figure 14. Stiffness Degradation over Cycles for Specimen SC-W-H

SUMMARY AND CONCLUSIONS

This paper presents the preliminary results from a research project, the overall goal of which is to develop knowledge-based design guidelines for safety related nuclear facilities subjected to combined accident thermal conditions and seismic loading. The project experimental and numerical investigations for SC (wall and wall pier) specimens are presented herein. The test matrix, the loading and heating protocol, instrumentation, and test set up for the specimens are briefly discussed. Specimen design and details, expected behavior, and preliminary experimental observations for SC specimens are also summarized.

Preliminary results from SC wall and wall piers indicate that thermal loads reduce the stiffness of walls. The reduction in stiffness is attributed to extensive concrete cracking due to non-linear thermal gradients through the thickness of the specimens. SC wall piers subjected to typical thermal loads (ranging from 300°F to 450°F for heating durations of 1 hour and 3 hour) did not exhibit significant degradation in strength and post-peak performance. Heated SC wall specimen also achieved its design strength, with a safety margin of 30%.

ACKNOWLEDGEMENTS

The research project is sponsored by US Department of Energy. The authors are grateful for their contribution to the project.

REFERENCES

ACI (2006). *Code Requirements for Nuclear Safety-Related Concrete Structures and Commentary*, ACI 349-06, American Concrete Institute, Farmington Hills, MI.

AISC (2015). *Specification for Safety-Related Steel Structures for Nuclear Facilities Including Supplement No. 1*. American Institute of Steel Construction. *AISC N690s1*. Chicago, IL, 2015.

ASCE (2005). *Seismic Design Criteria for Structures, Systems, and Components in Nuclear Facilities*, ASCE/SEI 43-05, American Society of Civil Engineers, Reston, VA, 2005.

Bhardwaj, S.R., Varma, A.H., and Sener, K.C. (2015). "On the Calculation of Design Demands for Accident Thermal Loading Combination." Transactions of SMiRT 23 in Manchester, UK, Paper ID 850, *IASMIRT*, North Carolina State University, Raleigh, NC, pp. 1-10, http://smirt23.uk/attachments/SMiRT-23_Paper_850.pdf

Epackachi, S., Nguyen, N., Kurt, E., Whittaker, A. and Varma, A. (2015). "In-Plane Seismic Behavior of Rectangular Steel-Plate Composite Wall Piers." *Journal of Structural Engineering*, ASCE, http://dx.doi.org/10.1061/(ASCE)ST.1943-541X.0001148.

Kitajima, Y., Miyagawa, T., Hirako, S., Kojima, I., Hirama T., and Akase, T., (2015). "Applicability Evaluation of Steel Plate Reinforced Concrete Structure to Primary Containment Vessel of BWRs: (4) Shear Loading Test of Steel Plate Reinforced Concrete Structure Under High Temperature Conditions." Transactions of SMiRT 23 in Manchester, UK, Paper ID 277, *IASMIRT*, NCSU.

Kurt, E.G., Varma, A.H., Booth, P.N. and Whittaker, A., (2016). "In-plane Behavior and Design of Rectangular SC Wall Piers Without Boundary Elements." *Journal of Structural Engineering*, Vol. 142, No. 6, ASCE, Reston, VA. http://dx.doi.org/10.1061/(ASCE)ST.1943-541X.0001481

Luna, B., Rivera, J.P., Whittaker, A. (2015). "Seismic behavior of low-aspect-ratio reinforced concrete shear walls". *ACI Structural Journal*, Vol. 112(5), pp. 593-604, September 2015. DOI: 10.14359/51687709

Ozaki, M., Akita, S., Oosuga, H., Nakayama, T. and Adachi, N. (2004). "Study on Steel Plate Reinforced Concrete Panels Subjected to Cyclic In-Plane Shear," *Nuclear Engineering and Design*, Vol. 228, pp. 225–244.

Sener, K.C., Varma, A.H., and Bhardwaj, S.R. (2015). "Accident Thermal Loading Effects on Seismic Behaviour of Safety-Related Nuclear Structures." Transactions of SMiRT 23 in Manchester, UK, Paper ID 701, *IASMIRT*, North Carolina State University, Raleigh, NC, pp. 1-10.

Sener, K.C., Varma, A.H., and Chu, M. (2017). "On the Performance of Steel-Concrete Composite (Sc) Modular Structures for Seismic and Accident Thermal Conditions" Transactions of SMiRT 24 in Busan, South Korea, Paper ID 06-15-05, *IASMIRT*.

Seo, J., Varma, A.H., Sener, K. and Ayhan, D. (2016). "Steel-Plate Composite (SC) Walls: In-Plane Shear Behavior, Database, and Design." *Journal of Constructional Steel Research*, Elsevier Science, Volume 119, Pages 202-215, http://dx.doi.org/10.1016/j.jcsr.2015.12.013

Varma, A.H., Zhang, K., Chi, H., Booth, P.N. and Baker, T. (2011). "In-Plane Shear Behavior of SC Walls: Theory vs. Experiment," *Transactions of the Internal Association for Structural Mechanics in Reactor Technology Conference, SMiRT-21, Div. X Paper 761*, New Delhi, India, IASMIRT, NCSU, Raleigh, NC, pp. 1–10.